Journal of Visualized Experiments

An approach to study shape-dependent transcriptomics at single-cell level

--Manuscript Draft--

Article Type:	Invited Methods Article - JoVE Produced Video
Manuscript Number:	JoVE61577R2
Full Title:	An approach to study shape-dependent transcriptomics at single-cell level
Section/Category:	JoVE Genetics
Keywords:	micropatterning; cell shape; adherent cell sorting; single-cell RNA sequencing; heart failure; cardiomyocyte
Corresponding Author:	Payam Haftbaradaran Esfahani Karolinska Institutet Department of Medicine Huddinge Huddinge, Stockholm SWEDEN
Corresponding Author's Institution:	Karolinska Institutet Department of Medicine Huddinge
Corresponding Author E-Mail:	payam.haftbaradaran@ki.se
Order of Authors:	Payam Haftbaradaran Esfahani
	Ralph Knöll
Additional Information:	
Question	**Response**
Please indicate whether this article will be Standard Access or Open Access.	Open Access (US$4,200)
Please indicate the **city, state/province, and country** where this article will be **filmed**. Please do not use abbreviations.	Stockholm, Stockholm, Sweden

TITLE:

An Approach to Study Shape-Dependent Transcriptomics at a Single Cell Level

AUTHORS AND AFFILIATIONS:

Payam Haftbaradaran Esfahani[1], Ralph Knöll[1,2]

[1]Department of Medicine, Integrated Cardio Metabolic Centre (ICMC), Heart and Vascular Theme, Karolinska Institutet, Huddinge, Sweden

[2]Bioscience Cardiovascular, Research and Early Development, Cardiovascular, Renal and Metabolism (CVRM), BioPharmaceuticals R&D, AstraZeneca, Gothenburg, Sweden

Email addresses of co-authors:

Payam Haftbaradaran Esfahani

(payam.haftbaradaran@ki.se)

Corresponding author:

Ralph Knöll

(ralph.knoell@astrazeneca.com)

KEYWORDS:

Micropatterning, cell shape, adherent cell sorting, single-cell RNA sequencing, heart failure, cardiomyocyte

SUMMARY:

This paper presents methods for growing cardiac myocytes with different shapes, which represent different pathologies, and sorting these adherent cardiac myocytes based on their morphology at a single cell level. The proposed platform provides a novel approach to high throughput and drug screening for different types of heart failure.

ABSTRACT:

Different types of cardiac hypertrophy have been associated with an increased volume of cardiac myocytes (CMs), along with changes in CM morphology. While the effects of cell volume on gene expression are well known, the effects of cell shape are not well understood. This paper describes a method that has been designed to systematically analyze the effects of CM morphology on gene expression. It details the development of a novel single-cell trapping strategy that is then followed by single-cell mRNA sequencing. A micropatterned chip has also been designed, which contains 3000 rectangular-shaped fibronectin micropatterns. This makes it possible to grow CMs in distinct length:width aspect ratios (AR), corresponding to different types of heart failure (HF). The paper also describes a protocol that has been designed to pick up single cells from their pattern, using a semi-automated micro-pipetting cell picker, and individually inject them into a separate lysis buffer. This has made it possible to profile the transcriptomes of single CMs with defined geometrical morphotypes and characterize them according to a range of normal or pathological conditions: hypertrophic cardiomyopathy (HCM) or afterload/concentric versus dilated cardiomyopathy (DCM) or preload/eccentric. In

summary, this paper presents methods for growing CMs with different shapes, which represent different pathologies, and sorting these adherent CMs based on their morphology at a single-cell level. The proposed platform provides a novel approach to high throughput and drug screening for different types of HF.

INTRODUCTION:

According to the World Health Organization, cardiovascular disease (CVD) is a major cause of morbidity and mortality worldwide. CVD dramatically affects the quality of people's lives and has a huge socioeconomic impact. Cardiomyopathies, such as HCM and DCM, are primary disorders of the heart muscle and major causes of HF have been associated with high morbidity and mortality. There are many causes of HF, including environmental effects, such as infections and exposure to toxins or certain drugs[8]. HF can also be caused by genetic predisposition, namely mutations[9]. It is believed that the changes in genetic composition that affect extracellular matrix (ECM) molecules, integrins or cytoskeletal proteins could be responsible for impaired mechanosensation and various types of cardiac disease[10].

The main feature of HCM is unexplained hypertrophy of the left ventricle[11], and sometimes of the right ventricle[12], and this frequently presents with predominant involvement of the interventricular septum. HCM is also characterized by diastolic dysfunction and myocyte disarray and fibrosis[13]. In most cases, the contractile apparatus of the heart is affected by mutations in sarcomeric proteins, leading to increased contractility of the myocytes[14]. In contrast, DCM is characterized by dilatation of one, or both, ventricles and has a familial etiology in 30% to 50% of cases[15]. DCM affects a wide range of cellular functions, leading to impaired contraction of the myocytes, cell death and fibrotic repair[16].

Genetics has shown that certain types of mutations force single CMs to adopt specific shape characteristics during HCM[3], namely square-shaped cells with a length:width AR that is almost equal to 1:1[4] (AR1). The same is true for DCM, with elongated cells with an AR that is almost equal to 11:1 (AR11). In addition, HF can be caused by increased afterload (e.g., in hypertension). In these cases, hemodynamic demands force CMs to take on square shapes, according to the Laplace's law, and the AR changes from 7:1[5] (AR7) to 1:1[6,7]. HF can also be caused by an increase in preload (e.g., in conditions that lead to volume overload). When this happens, the biophysical constraints force CMs to elongate and the AR changes from 7:1 to 11:1.

Signaling activity at membranes depend on global cell geometry parameters, such as the cellular AR, size, the membrane surface area and the membrane curvature[18]. When neonatal rat CMs were plated on substrates that were patterned to constrain the cells in a specific length:width AR, they demonstrated the best contractile function when the ratios were similar to the cells in a healthy adult heart. In contrast, they performed poorly when the ratios were similar to those of myocytes in failing hearts[19]. In the early stages of hypertrophy, cells become wider, as reflected by an increase in the cross-sectional area. HF occurs in the later stages of hypertrophy and cells typically appear elongated. Therefore, it is not surprising that in vivo rat models of chronic hypertrophy have reported an increase in the left ventricular myocyte length

of around 30%[20], but adult CMs from transgenic mouse model that were acutely treated with hypertrophic stimuli in vitro demonstrated similar increases in cell width instead[21].

Single-cell RNA sequencing, which allows precise analysis of the transcriptome of single cells, is currently revolutionizing the understanding of cell biology. This technology was the preferred method when it came to answering the question of how did individual cell shapes affect gene expression. We compared single cells with different shapes, in particular with ARs of 1:1, 7:1 or 11:1. This was done by seeding the neonatal rat ventricular CMs onto a specially designed chip filled with the fibronectin-coated micropatterns[2] with defined ARs of 1:1, 7:1 or 11:1. The micropatterns were fabricated using photolithography technology. The micropatterns were coated by fibronectin, surrounded by cytophobic surface. Therefore, CMs will attach, spread and capture the defined AR of micropatterns by solely growing on the fibronectin substrate, while avoiding the cytophobic area. The micropatterns are not in a well-shaped format. Instead, the fibronectin level is exactly at the same height of the surrounding cytophobic area. This provided similar conditions to growing cells in a Petri dish, as there is no stress from the surrounding walls. In addition, the surface area of micropatterns with different ARs are equal.

There were two particularly important aspects of the experimental design, which led to the use of single-cell RNA sequencing instead of bulk RNA sequencing. First, only a few percentages of the micropatterns can be occupied by a single cell. Second, sometimes a single cell does not fully occupy the micropattern surface. Single cells that completely cover a micropattern surface must be picked for single-cell RNA analysis. Because only a subgroup of the plated cells on a chip satisfied both criteria, it was not feasible to simply trypsinize the whole chip and collect all the cells for bulk RNA sequencing. Qualified cells needed to be picked individually using a semi-automated cell picker.

It currently remains unknown whether CM shape, by itself, has an intra-functional impact on the myocardial syncytium. The main purpose of the methods proposed in this paper was to develop a novel platform to study whether cell shape per se had an impact on the transcriptome[17]. Although in vitro studies are different from in vivo studies, the purpose of this study was to investigate the effect of different cell shapes on gene expression, bearing in mind that comparing cells with different shapes in vivo is extremely demanding. These experiments were inspired by Kuo et al.[19], who used a similar approach and reported that they observed changes in physiological parameters due to changes in cell shape.

PROTOCOL:

All the procedures involving animals were in accordance with the regulations of the animal ethics committee of the Karolinska Institutet, Stockholm, Sweden.

1. Micro-patterned chip layout

1.1. Use a custom-designed chip (**Table of Materials**) (**Figure 1A**): a 19.5 mm x 19.5 mm coverslip with activated micropatterns, printed by photolithography on borosilicate glass.

NOTE: These micropatterns are surrounded by a cytophobic area. Therefore, a seeded cell can only attach and grow on one of these micropatterns and capture the AR of that micropattern. The chip is divided into three zones and each zone consists of micropatterns with a specific AR. The chip layout is shown in **Figure 1B**. The geometry of the defined ARs is presented in **Table 1**. Magnified fluorescent images of the different shapes of the fibronectin micropatterns are shown in the lower images in **Figure 1B**.

2. Coating micropatterned chips

2.1. Prepare 2x coating protein solution for each chip by adding 80 µg of fibronectin to 2 mL of phosphate-buffered saline ($PBS^{-/-}$).

2.2. Transfer a chip to a 35 mm Greiner Petri dish and immediately add 2 mL of $PBS^{-/-}$. Then add 2 mL of the 2x coating protein solution.

2.3. Incubate the chips at room temperature for 2 h.

2.4. Wash the coating solution by successive dilution steps with $PBS^{-/-}$. The chip surface should always be wet. Then, replace the PBS with 2 mL of plating medium and incubate at 37 °C until seeding cells.

3. Isolation of CMs

3.1. Prepare the plating medium by supplementing DMEM:M199 (4:1) with 10% horse serum, 4% fetal bovine serum, 2% HEPES (1 M) and 1% penicillin/streptomycin (10,000 U/mL)[22].

3.2. Dissect the tissue from the left ventricle of 2-day-old neonatal rat hearts and transfer to a 10 cm dish containing PBS. Cut the tissue into approximately 1 mm^3 pieces.

3.3. Transfer the harvested tissue into a rotor-cap tube, equipped with a rotor in the cap for tissue dissociation (**Table of Materials**). Let the tissue settle down and then carefully remove the supernatant.

3.4. Add 2.5 mL of the mixture of enzyme mix 1 and 2, prepared using the Neonatal Heart Dissociation Kit (**Table of Materials**), to the C Tube and close the cap tightly.

3.5. Insert the rotor-cap tube onto the sleeve of the dissociator, equipped with heaters (**Figure 2A and B**) (**Table of Materials**). Run the incubation program 37C_mr_NHDK_1 (**Figure 2C**), which lasts about an hour.

3.6. While the incubation program is running, prepare PEB buffer containing 2 mM EDTA and 0.5% bovine serum albumin (BSA) in PBS, pH 7.2, and keep it at 4 °C.

3.7. After termination of the incubation program, detach the rotor-cap tube (**Figure 2D**) and add 7.5 mL of pre-warmed plating medium.

3.8. Resuspend the sample and filter the cell suspension using a 70 µm strainer.

3.9. Wash the strainer with another 3 mL of plating medium.

3.10. Centrifuge the cell suspension at 600 x *g* for 5 min. Aspirate the supernatant completely.

3.11. Resuspend the cell pellet in 60 µL of cold PEB buffer.

3.12. Add 20 µL of Neonatal Cardiomyocyte Isolation Cocktail (**Table of Materials**), containing micron-sized beads that target non-CMs.

3.13. Add 20 µL of Anti-Red Blood Cell beads (**Table of Materials**).

3.14. Mix the suspension and incubate at 4 °C for 15 min.

3.15. Add 400 µL of PEB buffer.

3.16. Apply the cell suspension onto the LD column (**Table of Materials**), which has been inserted vertically into a magnet stand and washed well with PEB buffer.

3.17. Collect unlabeled cells and wash column with 0.5 mL of PEB buffer.

3.18. Add 8 mL of plating medium and transfer the cell suspension into a 75-cm^2 uncoated culture flask and incubate at 37 °C for 1.5 h. The remaining non-CMs will start to adhere to the uncoated cell culture and the cell suspension will be enriched by the CM population.

4. Patterning CMs

NOTE: We compared single CMs with ARs of 1:1, 7:1 or 11:1. This is done by seeding the isolated neonatal rat CMs onto a specially designed chip filled with fibronectin-coated micropatterns with defined ARs of 1:1, 7:1 or 11:1. The micropatterns were coated by fibronectin, surrounded by cytophobic surface. Therefore, CMs will attach, spread and capture the defined AR of micropatterns by solely growing on the fibronectin substrate. Pattern the isolated CMs according to the following steps.

4.1. Transfer the cell suspension to a 15 mL tube, count the cells and dilute to a concentration of 100,000 cells per mL by adding appropriate plating medium.

4.2. Add 2 mL of cell suspension onto the chip, which has already been submerged in 2 mL of warm plating medium inside a 35 mm Greiner Petri dish.

4.3. Incubate the dish at 37 °C with 5% CO_2 to let the CMs attach to the fibronectin-coated micropatterns and allow each CM to acquire the AR of its substrate micropattern.

4.4. After 18 h, check the chip. If most of the cells have attached, detach and remove the debris and dead cells that are attached to the patterned cell. Do this by removing the plating medium and gently adding $PBS^{-/-}$ dropwise, starting from the center of the chip then moving towards the sides. Repeat 2 times.

4.5. Aspirate the PBS with fresh maintenance medium by supplementing DMEM:M199 (4:1) with 4% horse serum, 4% fetal bovine serum, 2% HEPES (1 M) and 1% penicillin/streptomycin (10,000 U/mL).

5. Picking adherent CMs

NOTE: After a culturing period of 72 hours, patterned single CMs are picked from their fibronectin micropatterns using a semi-automated cell picker (**Table of Materials**) (**Figure 3**). The cell picker uses a software[23] to control the motorized stage (**Figure 3A**). A 70 µm glass microcapillary (**Figure 3B**) is used to pick and inject the patterned neonatal rat CMs. The cell picker sorts adherent cells by generating a vacuum and injecting the cells by applying pressure. The vacuum in syringe number 1 is applied by pulling the syringe using the syringe pump (**Figure 3C**). The hydrostatic pressure is based on gravity and induced by placing syringe number 2 at a distance of 87 cm over the microscope desk. Syringes 1 and 2 are respectively connected via PTFE tubes, to valves 1 and 2, which are embedded in the control unit (**Figure 3D**). The PTFE tubes are completely filled with RNase-free water. The picked single cell is then injected to the polymerase chain reaction (PCR) tube, containing 3.55 µL of lysis buffer.

5.1. After a culturing period of 72 hours, remove the old medium and gently flush the chip surface with warm $DPBS^{-/-}$.

5.1.1. Keep the dish flat and aspirate the old medium gently with a 1000 µL pipette from one side of the dish. Make sure that the chip remains wet at all times.

5.1.2. Add 2 mL of $DPBS^{-/-}$ gently and drop-wise detach most of the dead cells that are attached to the patterned cells, starting from the center of the chip and then moving to its sides.

5.1.3. Aspirate most of the DPBS to remove as many detached floating cells as possible, starting from the center of the chip and then moving to the sides.

5.1.4. Repeat steps 5.1.2 and 5.1.3 once more.

5.2. Use angled forceps to grab the edge of the chip and immediately transfer it to a new sterile 35 mm Greiner Petri dish to reduce the number of floating cells while picking.

5.3. Immediately add 1.5 mL of $DPBS^{-/-}$ so that the chip does not dry out.

5.4. Add 1.5 µL of Vibrant Dye Cycle green to visualize the nuclei of the live cells.

5.5. Place the chip in the center of the Greiner Petri dish by using the tip of the forceps.

5.6. Put a chamber (**Table of Materials**) over the chip. The chamber will fix the chip to the bottom of the dish, without blocking access to the cell patterns.

5.7. Mount the Greiner Petri dish onto the dish holder of the cell picker stage and insert the magnetic cap.

5.8. Calibrate the automated injection.

5.8.1. Locate the crosshair, which is engraved on the motorized stage in the middle of the image in the Live View window.

5.8.2. Focus on the crosshair and select the **Calibration for automated injection** button in the **Scanning and sorting** window.

5.9. Replace the $DPBS^{-/-}$ with 1.5 mL of $DPBS/trypsin^{-/-}$ (1:1) while the dish is on the stage, to loosen the cells from the fibronectin so that a fluidic vacuum can be used to pick the cells.

5.10. Scan the whole chip using the **Scanning** tab in the **Scanning and sorting** window. Locate the top left corner of the chip in the field of view and click on **Get current microscope position** in the top left corner row.

5.10.1. Then, move the motorized stage to the bottom right corner of the chip. Focus the microscope and click on **Get current microscope position** in the bottom right corner row.

5.11 Click on the **Set sharpest plane** button and on the popped up window click on the **Go to the top right corner**. Focus the microscope and click on **Go to the bottom left corner** and set the focus. When done click the **Finish** button and start scanning.

5.12. When the scanning is terminated, go to the **Analyzing** tab and select the single cells that pass the study criteria.

5.13. Make sure that the glass microcapillary is in the middle of the microscope's live view.

5.14. Control the syringe pump using the **Pump** window of the software. Create a vacuum by withdrawing 4 mL from a 50 mL number 1 syringe, which has a diameter of 27 mm.

5.15. In the **Sorting** tab

5.15.1. Set the injection parameters of the valves. It was calculated that the injection volume that delivered a picked single cell was 1 µl, if valve 2 was opened for 120 milliseconds and then valve 1 opened for 20 was milliseconds after a time lapse of 200 milliseconds. Due to the elasticity of the tubes, open valve 1 to stop injecting the flow.

5.15.2. Set the pick-up parameters of the valves. It was calculated that if valve 1 was opened for 20 milliseconds and then valve 2 was opened for 10 milliseconds, after a time lapse of 10 milliseconds, most of the patterned cells can be picked up. This is because their fibronectin bindings were loosened after being treated by trypsin.

5.15.3. Click on the **Compute the path** button. The software computes the fastest path from cell to cell, to pick up and inject the selected cells throughout the chip.

5.15.4. Focus the microscope on a patterned cell on the chip surface.

5.15.5. Using the joystick, move the microcapillary down carefully, so that the sharpest image of the tip of the microcapillary can be obtained without touching the cell.

5.15.6. Click the **Set** button in the **Micropipette offset** section. A new window will pop up, showing the microcapillary cross section. Click on the exact center of the capillary. The software will then record the tip offset of the capillary in the x, y and z coordinates.

5.15.7. Launch sorting using the **Start sorting** button.

REPRESENTATIVE RESULTS:

Tissue was dissected from the left ventricle of the 2-day-old neonatal rat hearts and divided into single cells. Then the enriched CMs were seeded on a chip containing fibronectin patterns with distinct ARs. After 72 hours of culturing, the medium was replaced by 1:1000 Vibrant Dye Cycle green in $DPBS^{-/-}$ for 2 min to visualize the nuclei of the live cells. Next, the cells were treated with $DPBS^{-/-}$/trypsin (1:1) to loosen the cells from the fibronectin, so that a fluidic vacuum could be used to facilitate cell picking. Meanwhile, the entire chip was scanned at a magnification of 10x, using an inverted microscope connected to the cell picker. This was carried out before the cells became rounded due to trypsin treatment. The qualified cells were selected, based on the scanned image, and their coordinates were saved in the cell picker software. The micropatterns were only selected if they contained a mononucleated single cell and only when the cell fully covered its fibronectin micropattern. The cell sorter picked the selected cells one by one and each single cell that was successfully picked was immediately injected into an individual PCR tube and placed on the microscope stage. Each PCR tube contained 3.55 µL of lysis buffer (**Table 2**). The sorting process, which started with removing the media, was completed within 40 minutes. The complementary deoxyribonucleic acid (cDNA) synthesis, PCR pre-amplification and purification were performed on the lysed single cells, based on the Smart-Seq2 protocol[24] (**Table 3**). The quality of the purified cDNA was checked by an automated electrophoresis analyzer. The electropherogram of the pre-amplified cDNA of one picked single cell is presented in **Figure 4**. The RNA-Seq libraries were prepared according to the Smart-Seq2 protocol[24].

To observe the sarcomere structure of the patterned CMs, the patterned CMs were stained with sarcomeric α-actinin antibody. The cells were incubated with Donkey Anti-Mouse IgG Alexa Fluor 488 1:800 for 1 hour at room temperature for the secondary staining. Nuclei were stained with 1 µg/mL DAPI. Immunofluorescent images were acquired with an inverted confocal microscope, using a 63x oil-immersion (NA 1.4) objective (**Figure 5**).

FIGURE LEGENDS:

Figure 1. Layout of the chip with fibronectin micropatterns. (**A**) Image of the custom-designed chip. The chip is a 19.5 mm x 19.5 mm coverslip with fibronectin micropatterns, printed by photolithography on a borosilicate glass. (**B**) Chip layout. The chip is divided to three zones and each zone consists of fibronectin micropatterns with specific AR. Fluorescent images of different shapes of fibronectin micropatterns are shown in magnified view for each zone. This figure has been modified from "*supplementary material 1*" by Haftbaradaran Esfahani et al.[2], used under http://creativecommons.org/licenses/by/4.0/ .

Figure 2. Dissociator equipped with heaters apparatus. (**A**) The entire dissociator instrument used for the fully automated dissociation of 2-day-old neonatal rat left ventricles. (**B**) Heating unit. (**C**) Rotor-cap tube. (**D**) Ready-to-use programs for a fully automated workflow of tissue dissociation.

Figure 3. Cell picker apparatus. (**A**) Enlarged view of the motorized stage of the cell picker. A Petri-dish holder and 80 holes for 10 PCR strips and a hole for calibration crosshair is embedded on the stage. (**B**) Enlarged view of a glass microcapillary. (**C**) The syringe pump. (**D**) The control unit, which controls the opening and closing time window of valves 1 and 2, mounted inside the control unit.

Figure 4. The electropherogram of the pre-amplified cDNA of one picked single cell. 19 PCR cycles of pre-amplification was used to obtain 15 µL of 1 ng/µL purified cDNA yield. A clear band in gel-like densitometry plot is observed which corresponds to the peak at 1852 bp in the electropherogram. The average size of fragments is 1588 bp. Moreover, the small amount of fragments that are shorter than 300 bp indicates a good cDNA library.

Figure 5. Immunofluorescent staining of α-actinin sarcomeric structure (green) and nucleus (blue) of patterned CMs with different ARs. The chromatin was stained by DAPI.

Table 1: Geometry of patterned CMs.

Table 2: Single cell custom lysis buffer.

Table 3: Reverse transcription (RT) mix for one RT reaction to synthesize first-strand cDNA from the lysate of a single CM.

DISCUSSION:

This study used single-cell RNA sequencing, which is a novel and powerful technology that can detect the transcriptome of single cells. It was combined with an innovative approach to culturing single CMs, so that they took on different ARs that, otherwise, could only have been observed in vivo.

The study had some limitations. For example, neonatal CMs had to be used to generate different morphotypes, as it is exceptionally challenging to culture enough vital adult CMs for 72 hours in defined shapes. Furthermore, CMs were cultured for 72 hours ex vivo, which might have had an impact on the gene expression pattern. However, this culturing was necessary, so that the cells could form specific morphotypes. Moreover, only single cells that were mononucleated and fully covered the fibronectin micropattern were selected for sorting. Patterned cells on each chip must be sorted merely in one round of sorting. Finally, about 50 cells that is roughly one-third of the selected cells were successfully picked up from each chip. There are two reasons that restricted the number of successfully picked cells. First, some cells were too tightly attached to the fibronectin pattern and the pickup flow was not forcible enough to successfully pick them up. Second, due to the trypsin treatment, the attachment between some cells and fibronectin became too loose. Consequently, these cells were pushed away from their fibronectin micropatterns, when the microcapillary approached them, and they were not picked up. The authors do not claim that this setup is the same as an in vivo environment, but it proved to be a viable approach to answering the research question.

The proposed method is applicable on different cell types (e.g., for hiPS-CMs). However, the following factors should be optimized to study other cell-types. Suitable ECM adhesive molecules for attachment of the specific cell-type should be used for coating the micropatterns. The geometry of the micropatterns should be modified according to the study question and cell-type. The culturing period can be modified based on the study question. The detachment reagent and its incubation time should be optimized precisely for the study cell-type. For instance, Accutase can be used instead of TryplE for detachment of embryonic and neuronal stem cells. The opening time parameters of the valves should be scrutinized to pick cells successfully, but gently. In summary, we engineered a novel platform to study cell shape that can provide a valuable resource for researchers in the field. In this context, we designed an experimental approach that mimicked in vitro characteristic shapes imposed on CM in vivo by hemodynamic constraints to identify the interplay between cellular architecture and gene expression. We also report the development of a novel platform to study HF in vitro and the identification of cell shape as a powerful determinant of gene expression. This is a novel observation with far-reaching implications for biology and medicine.

REFERENCES:

1 Heineke, J., Molkentin, J. D. Regulation of cardiac hypertrophy by intracellular signalling pathways. *Nature Reviews Molecular Cell Biology.* **7** (8), 589-600 (2006).

2 Haftbaradaran Esfahani, P. et al. Cell shape determines gene expression: cardiomyocyte morphotypic transcriptomes. *Basic Research in Cardiology.* **115** (1), 7 (2019).

3 Kontrogianni-Konstantopoulos, A., Benian, G., Granzier, H. Advances in Muscle Physiology and Pathophysiology 2011. *Journal of Biomedicine and Biotechnology.* **2012**, 930836 (2012).
4 Hill, J. A., Olson, E. N. Cardiac plasticity. *New England Journal of Medicine.* **358** (13), 1370-1380 (2008).
5 Bray, M. A., Sheehy, S. P., Parker, K. K. Sarcomere alignment is regulated by myocyte shape. *Cell Motility and the Cytoskeleton.* **65** (8), 641-651 (2008).
6 Benjamin, I. J., Schneider, M. D. Learning from failure: congestive heart failure in the postgenomic age. *Journal of Clinical Investigation.* **115** (3), 495-499 (2005).
7 Opie, L. H., Commerford, P. J., Gersh, B. J., Pfeffer, M. A. Controversies in ventricular remodelling. *Lancet.* **367** (9507), 356-367 (2006).
8 Braunwald, E. Cardiomyopathies: An Overview. *Circulation Research.* **121** (7), 711-721 (2017).
9 Knoll, R. et al. The cardiac mechanical stretch sensor machinery involves a Z disc complex that is defective in a subset of human dilated cardiomyopathy. *Cell.* **111** (7), 943-955 (2002).
10 Frangogiannis, N. G. The Extracellular Matrix in Ischemic and Nonischemic Heart Failure. *Circulation Research.* **125** (1), 117-146 (2019).
11 Marian, A. J., Braunwald, E. Hypertrophic Cardiomyopathy: Genetics, Pathogenesis, Clinical Manifestations, Diagnosis, and Therapy. *Circulation Research.* **121** (7), 749-770 (2017).
12 Mozaffarian, D., Caldwell, J. H. Right ventricular involvement in hypertrophic cardiomyopathy: a case report and literature review. *Clinical Cardiology.* **24** (1), 2-8 (2001).
13 Olsson, M. C., Palmer, B. M., Stauffer, B. L., Leinwand, L. A., Moore, R. L. Morphological and functional alterations in ventricular myocytes from male transgenic mice with hypertrophic cardiomyopathy. *Circulation Research.* **94** (2), 201-207 (2004).
14 Toepfer, C. N. et al. Hypertrophic cardiomyopathy mutations in MYBPC3 dysregulate myosin. *Science Translational Medicine.* **11** (476) (2019).
15 McKenna, W. J., Maron, B. J., Thiene, G. Classification, Epidemiology, and Global Burden of Cardiomyopathies. *Circulation Research.* **121** (7), 722-730 (2017).
16 Schultheiss, H. P. et al. Dilated cardiomyopathy. *Nature Reviews Disease Primers.* **5** (1), 32 (2019).
17 Knoll, R. A role for membrane shape and information processing in cardiac physiology. *Pflugers Arch.* **467** (1), 167-173 (2015).
18 Rangamani, P. et al. Decoding information in cell shape. *Cell.* **154** (6), 1356-1369 (2013).
19 Kuo, P. L. et al. Myocyte shape regulates lateral registry of sarcomeres and contractility. *American Journal of Pathology.* **181** (6), 2030-2037 (2012).
20 Gerdes, A. M., Onodera, T., Wang, X., McCune, S. A. Myocyte remodeling during the progression to failure in rats with hypertension. *Hypertension.* **28** (4), 609-614 (1996).
21 Kehat, I. et al. Extracellular signal-regulated kinases 1 and 2 regulate the balance between eccentric and concentric cardiac growth. *Circulation Research.* **108** (2), 176-183 (2011).
22 Sreejit, P., Kumar, S., Verma, R. S. An improved protocol for primary culture of cardiomyocyte from neonatal mice. In Vitro Cellular & Developmental Biology – Animal. **44** (3-4), 45-50 (2008).

23 Kornyei, Z. et al. Cell sorting in a Petri dish controlled by computer vision. *Scientific Reports.* **3** 1088 (2013).
24 Picelli, S. et al. Full-length RNA-seq from single cells using Smart-seq2. *Nature Protocols.* **9** (1), 171-181 (2014).
25 Schmick, M., Bastiaens, P. I. H. The interdependence of membrane shape and cellular signal processing. *Cell.* **156** (6), 1132-1138 (2014).

Figure 1 (Pdf format)

Click here to access/download;Figure;Figure 1.pdf

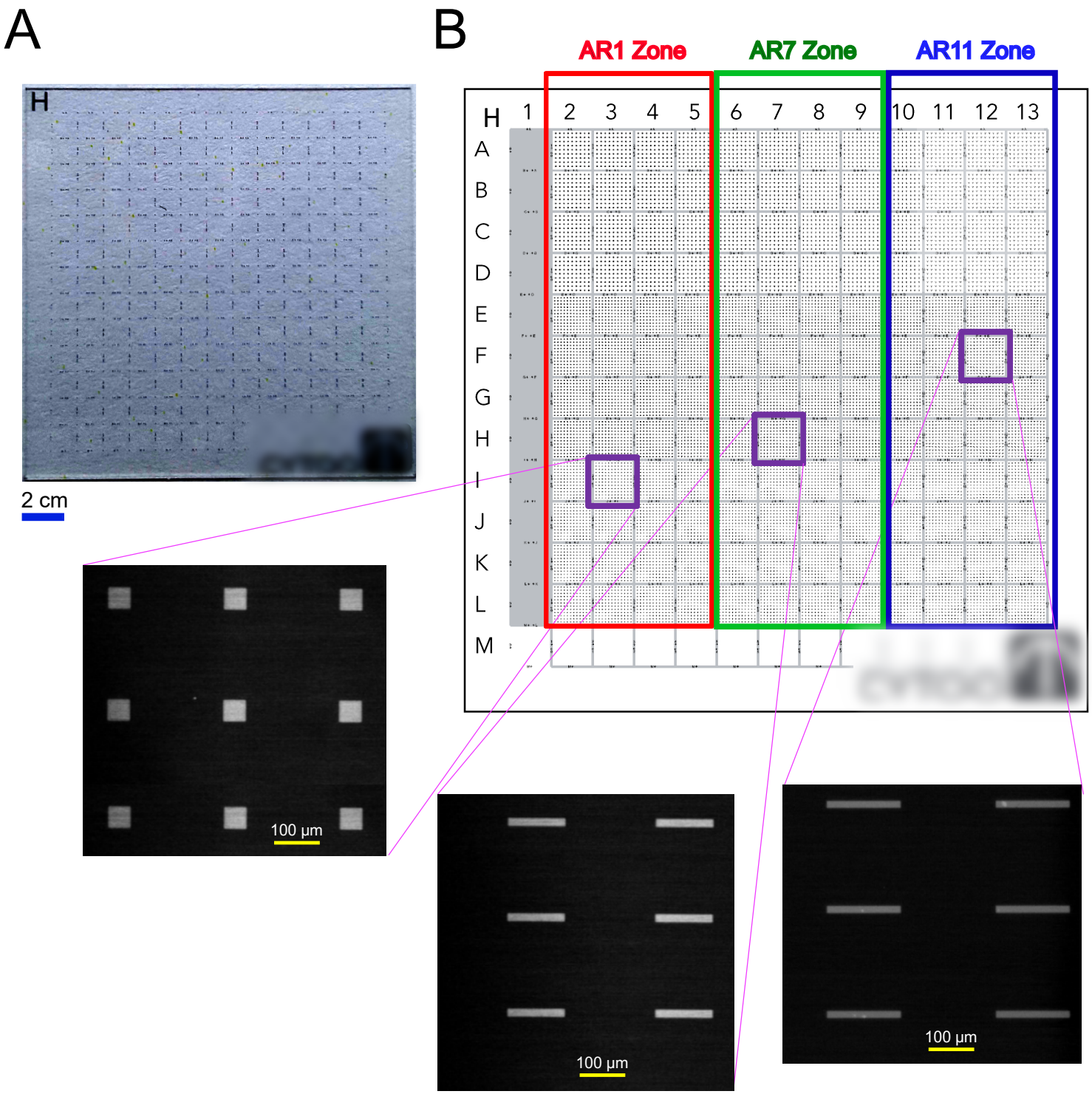

Figure 2 (Pdf format) Click here to access/download;Figure;Figure 2.pdf

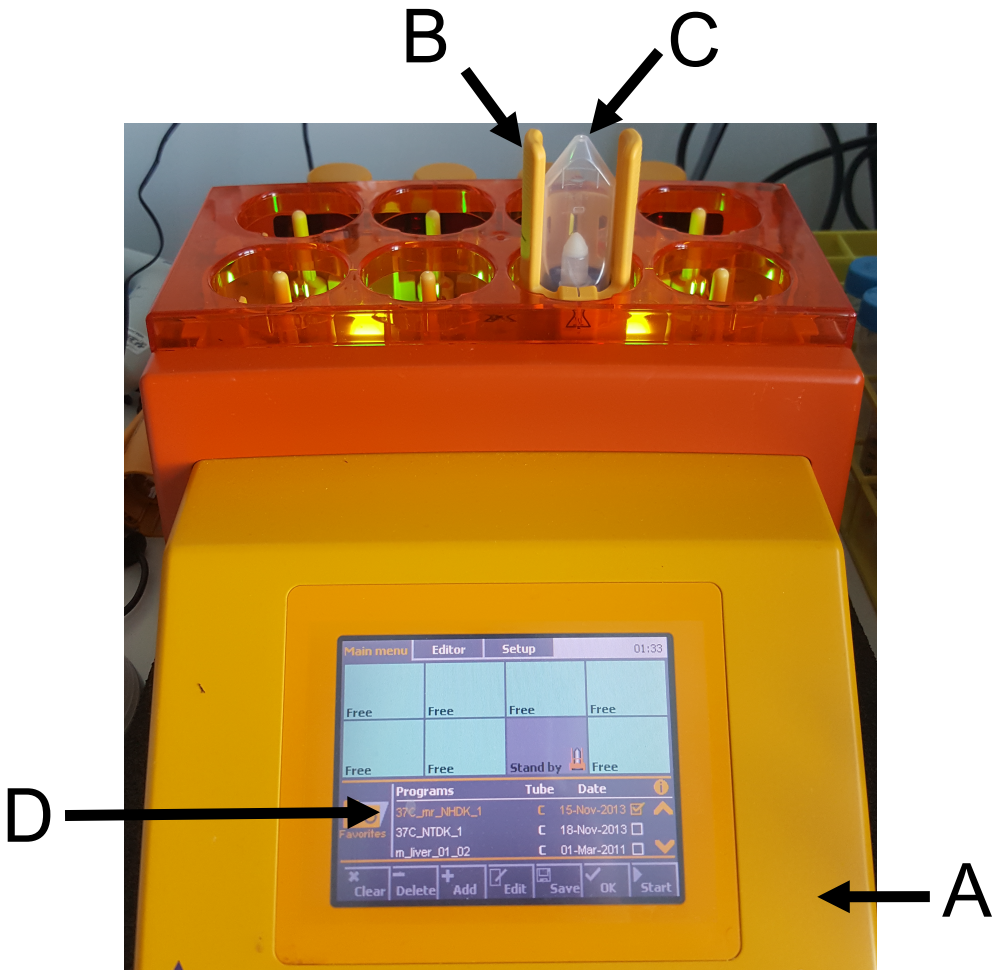

Figure 3 (Pdf format) Click here to access/download;Figure;Figure 3.pdf

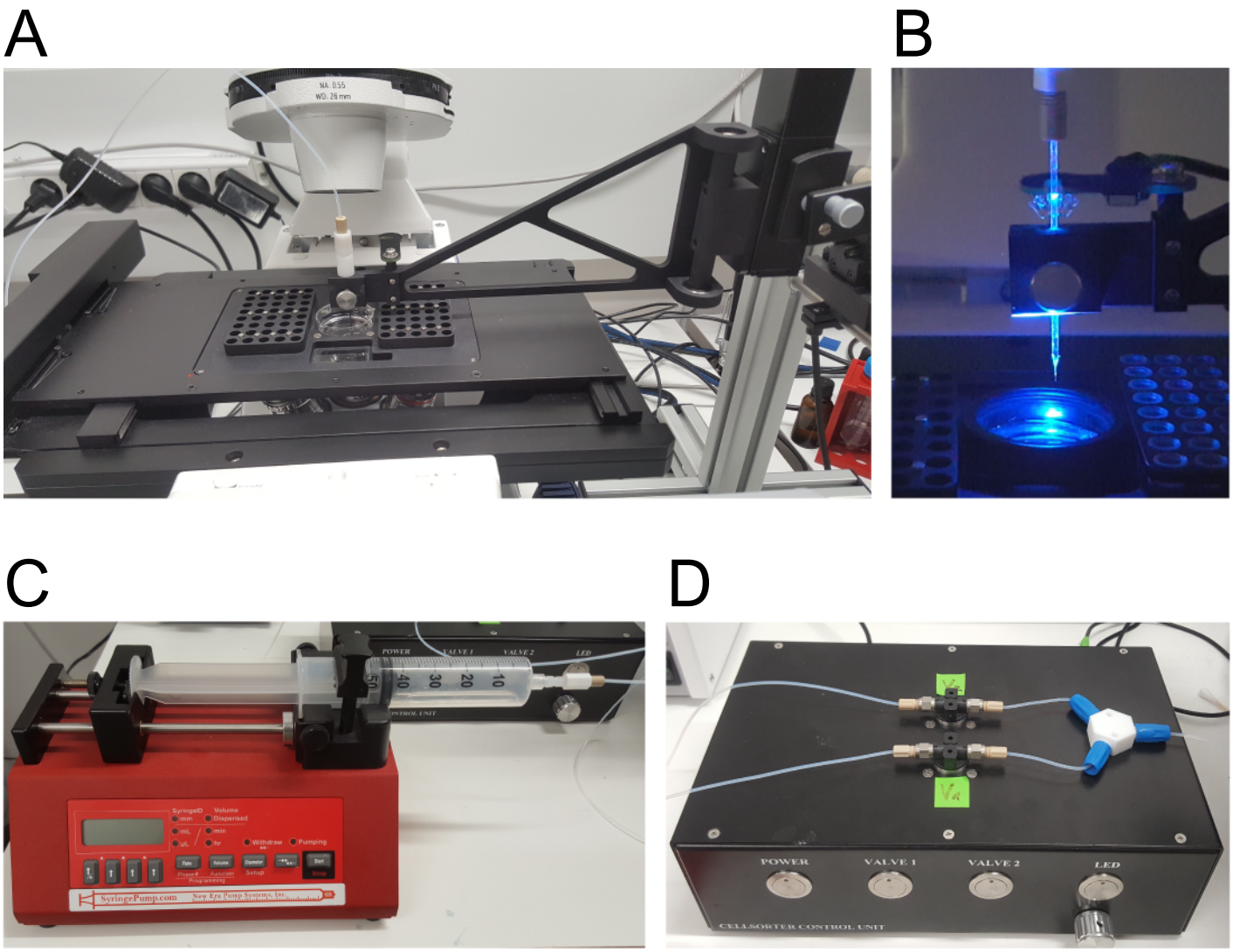

Figure 4 (Pdf format) Click here to access/download;Figure;Figure 4.pdf

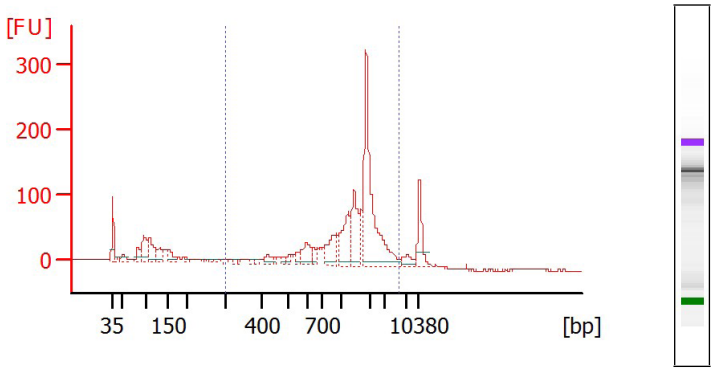

Region table for sample:

From [bp]	To [bp]	Corr. Area	% of Total	Average Size [bp]	Size distribution in CV [%]	Conc. [pg/µl]	Molarity [pmol/l]
300	6,000	1,506	75	1,588	55.2	1,026.7	1,527.8

Figure 5 (Pdf format)

Click here to access/download;Figure;Figure 5.pdf

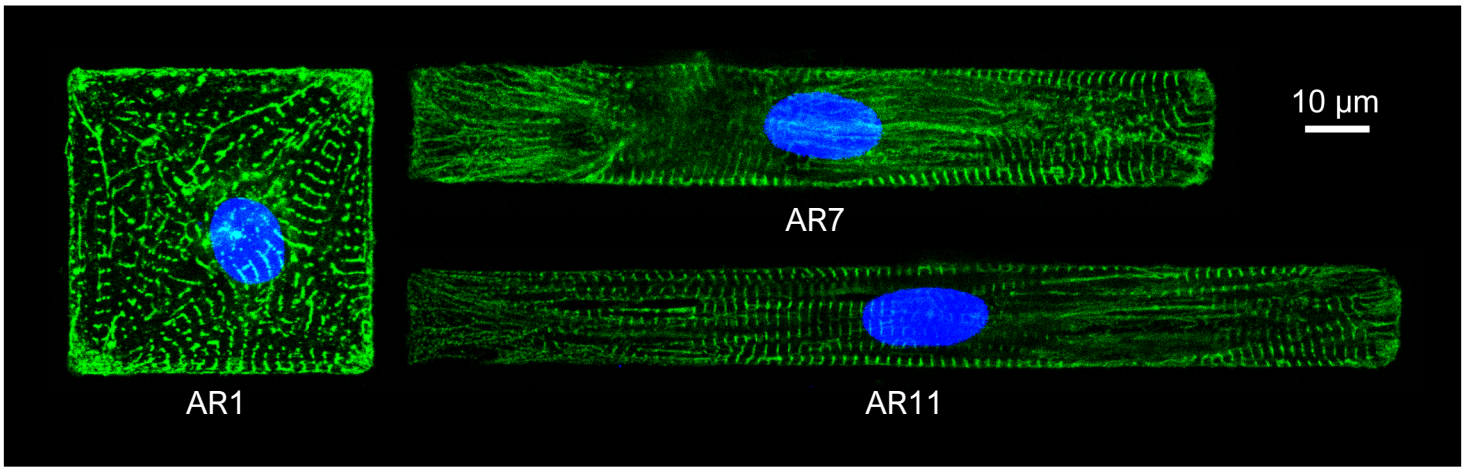

Figure 1 (Vector image format)

Click here to access/download

Video or Animated Figure

Figure 1.ai

Figure 2 (Vector image format)

Figure 3 (Vector image format)

Click here to access/download

Video or Animated Figure

Figure 3.svg

Figure 4 (Vector image format)

Figure 5 (Vector image format)

Table 1. Geometry of patterned CMs

Morphotype	AR	Length (μm)	Width (μm)	Fibronectin area (μm^2)
AR1	1:1	47	47	2209
AR7	7:1	126	18	2268
AR11	11:1	155	14	2170

Table 2. Single cell custom lysis buffer.

Component	Volume (µL)
Nucleas-free water	0.65
(0.4% vol/vol) Triton X-100	1.8
dNTP mix (25 mM)	0.8
RNase inhibitor (40 U μL^{-1})	0.1
Oligo-$dT_{30}VN$ oligonucleotides (100 µM)	0.1
ERCC RNA Spike-In Mix (2.5×10^{5} dilution)	0.1
Injected single cell	1
Total volume	4.55

Table 3. Reverse transcription (RT) mix for one RT reaction to synthesize first-strand cDNA from the

Component	Volume (µL)
Superscript II first-strand buffer (5x)	2
DTT (100 mM)	0.5
Betaine (5 M)	2
$Mgcl_2$ (1 M)	0.1
RNase inhibitor (40 U μL^{-1})	0.25
Superscript II reverse transcriptase (200 U µL-1)	0.5
TSO (100 µM)	0.1
Total volume	5.45

lysate of a single CM.

Table of Materials

Name of Material/ Equipment	Company	Catalog Number	Comments/Description
2100 Bioanalyzer Instrument	Agilent Technologies	G2939BA	Automated electrophoresis analyzer
Anti-Red Blood Cell MicroBeads	Miltenyi Biotec	130-109-681	
Axio Observer microscope	Zeiss	Z1	Inverted microscope
Betaine solution (5 M)	Sigma-Aldrich, MERCK	B0300	
CellSorter	CELLSORTER	https://www.singlec	Cell picker
CYTOOchamber	CYTOO	30-010	Custom-designed chip
CYTOOchip	CYTOO	10-950-00-18	Chamber
DMEM	Thermo Fisher Scientific	31966-021	high glucose, GlutaMAX Supplement
dNTP mix (25 mM)	Thermo Fisher Scientific	R1122	
Donkey Anti-Mouse IgG Alexa Fluor 488	Abcam PLC	ab150105	
DTT (100 mM)	Thermo Fisher Scientific	18064071	
ERCC RNA Spike-In Mix	Thermo Fisher Scientific	4456740	
Fetal Bovine Serum	Thermo Fisher Scientific	10082-147	
Fibronectin	Sigma-Aldrich, MERCK	F4759	
gentleMACS C Tube	Miltenyi Biotec	130-093-237	Rotor-cap tube
gentleMACS Octo Dissociator with Heaters	Miltenyi Biotec	130-096-427	Dissociator with heater
Greiner CELLSTAR Petri dish	Sigma-Aldrich, MERCK	P6987	
HEPES (1 M)	Thermo Fisher Scientific	15630-056	
Horse Serum	Sigma-Aldrich, MERCK	H0146	
LD column	Miltenyi Biotec	130-042-901	
Medium 199	Thermo Fisher Scientific	31150-022	
NE-1000 syringe pump	New Era Pump Systems	NE-1000	Syringe pump
Neonatal Cardiomyocyte Isolation Cocktail, rat	Miltenyi Biotec	130-105-420	
Neonatal Heart Dissociation Kit, mouse and rat	Miltenyi Biotec	130-098-373	

Oligo-$dT_{30}VN$ oligonucleotides	IDT Technology	5’–AAGCAGTGGTATCAACGCAGAGTACT30VN-3’
RNAse inhibitor (40 U μL^{-1})	Clontech	2313A
sarcomeric α-actinin	Sigma-Aldrich, MERCK	EA-53
SP8 confocal microscope	Leica Microsystems	SP8 Confocal microscope
Superscript II first-strand buffer (5x)	Thermo Fisher Scientific	18064071
Superscript II reverse transcriptase (200 U µL-1)	Thermo Fisher Scientific	18064071
Triton X-100	Sigma-Aldrich, MERCK	T9284
TryplE Express enzyme, no phenol red	Thermo Fisher Scientific	12604013
TSO (100 µM)	QIAGEN	5’-AAGCAGTGGTATCAACGCAGAGTACATrGrG+G-3’
Vibrant Dye Cycle green	Thermo Fisher Scientific	V35004

Response to Reviewer #1:

Overall Comment:

"This paper by Esfahani and Knoll puts forward a methodology for growing cardiac myocytes into different morphologies and sorting based on this variety of morphologies. The most immediate application of this is in identifying cellular characteristics of these morphologies and defining their association with cardiomyopathic disease."

We thank the reviewer for her/his overall comments.

Major Points:

1. *"Introduction seems a bit out of order. The paragraph starting on line 52 would seem to go best after the subsequent 3 paragraphs."*

We completely agree with this reviewer's point and appreciate it. Therefore, we moved the aforementioned paragraph to the suggested place.
In addition, few other paragraphs reordered to create a concise flow of ideas.

2. *"In the Introduction, it seems a bit unclear when the authors are talking about "CMs" in a general sense, or whether they are related to human pathology or CMs from experimental models."*

We thank the reviewer for this comment. We updated the introduction accordingly by clarifying the CMs model, when we were talking about CMs.
However, in some parts, the statement is generally true, so we did not specified any model. For example, in paragraphs 3 and 4 of the introduction of the revised manuscript.
In paragraph 5 of the introduction of the tracked version of the revised manuscript, on line 91, the "CMs" is "neonatal rat CMs", as updated accordingly in the tracked version of revised manuscript.
In paragraph 5 of the introduction of the tracked version of the revised manuscript, on lines 97 and 98, the "CMs" are from "rat models of chronic hypertrophy", as updated accordingly in the tracked version of revised manuscript.

In paragraph 5 of the introduction of the revised manuscript, on line 99, the “CMs” are from “transgenic mouse model”, as updated accordingly in the revised manuscript.
In paragraph 6 of the introduction of the tracked version of the revised manuscript, on lines 116 and 117, the “CMs” are from “neonatal rat ventricular CMs”, as updated accordingly in the tracked version of revised manuscript.

3. *“Overall, the introduction and discussion seems under-cited.”*

We appreciate the reviewer’s concern. Therefore, the revised manuscript is now cited meticulously.

4. *“The majority of discussion of the CM shape change occurring with disease seems to be in intact cardiac tissue. I am curious what is known about the morphology of cardiomyopathy-associated CMs that are dissociated? Cultured in vitro? Is there evidence that this morphology changes in response to confounding factors? Expanding this may help set the rationale for the methodology.”*

We appreciate the reviewer’s point. We refer the reviewer to lines 138 to 141 of the tracked version of the revised manuscript in which we discussed that “*It currently remains unknown whether CM shape, by itself, has an intra-functional impact on the myocardial syncytium. The main purpose of the methods proposed in this paper was to develop a novel platform to study whether cell shape per se had an impact on the transcriptome*”. Therefore, we were interested in the causal effect of cell shape *per se.* In other words, our scientific question was that “*to which extent the effects, seen in different cardiomyopathies, are merely caused by cell morphology of that cardiomyopathy?”*

5. *“It would appear that the CYTOOchip is a custom-designed reagent needed for the experiment. While it may not be possible to include alternatives, it would be important to provide additional detail regarding how it is made to aid in broader use/application. In addition, there are a number of reagents which seem equally unique. It is critical to at least discuss how scientists might apply this protocol broadly that is not absolutely dependent on these specific reagents.”*

We appreciate the reviewer’s point. The CYTOOchips are commercially available and the micropatterns are in the activated format, ready to be coated with the adhesive

molecule of interest. As an instance, in this study, we used fibronectin, which is simply available. Therefore, no custom-designed reagent is needed for the experiment.

However, if a researcher is interested to print the micropatterns in own lab, we refer to Kuo et al approach[1] for more details, as that technique was not in the scope of our proposed workflow.

6. *"Could this protocol be adapted for other types of cells? CMs derived from induced pluripotent stem cells come to mind. This would greatly broaden applicability."*

We really appreciate the reviewer's point. Therefore, we added the response to this question to the revised discussion.

"*The proposed method is applicable on different cell types, for example, for hiPS-CMs. However, the following factors should be optimized, studying other cell-types. I) Suitable ECM adhesive molecule for attachment of the specific cell-type should be used for coating the micropatterns. II) The geometry of the micropatterns should be modified according to the study question and cell-type. III) The culturing period can be modified based on the study question. IV) The detachment reagent and its incubation time should be optimized precisely for the study cell-type. As an instance, Accutase can be used instead of TryplE for detachment of embryonic and neuronal stem cells. V) The opening time parameters of the valves should be scrutinized to pick cells successfully, but gently."*

7. *"Figure 1, micron bars are needed to demonstrate scale."*

We thank the reviewer for this point. We added the scale bar to figure 1 accordingly.

8. *"Figure 4, the legend could use a bit more detail and the electropherogram more clearly defined, including the gel band sizes."*

We thank the reviewer for this point. We added more detailed information to the legend of figure 4 accordingly.

9. *"Figure 5, what was the nuclear stain?"*

We thank the reviewer for this point. We added this information to the legend of the figure 5 accordingly. Chromatin was stained by DAPI.

References:

1 Kuo, P. L. *et al.* Myocyte shape regulates lateral registry of sarcomeres and contractility. *Am J Pathol.* **181** (6), 2030-2037, (2012).

Response to Reviewer #2:

Overall Comment:

“In this manuscript, the authors propose methods for culturing cardiomyocytes in different shapes, which represent distinct cardiac pathologies, with an ultimate goal to investigate the effect of different cell shapes on gene expression. While the manuscript is well written, and it clearly describes the method, a few points need to be clarified.”

We thank the reviewer for her/his overall comments.

Major Concerns:

1. *“The title of the manuscript is very misleading. The reader will expect to see also single-cell RNA sequencing data and shape-depend transcriptomics as a readout of the study. However, the described method only covers the cardiomyocytes isolation, culturing and sorting cells for single-cell sequencing purposes, but no actual sequencing data. I would suggest clarifying this in the title.”*

We appreciate the reviewer’s point. We amended the title to “*An approach to study shape-dependent transcriptomics at single-cell level*”.

2. *“Following the previous point, in the discussion, the authors state: "This study used single cell RNA sequencing, which is a novel and powerful technology that can detect the transcriptome of single cells." I disagree with this statement, and this is not what this particular study is showing.”*

We agree with the reviewer’s concern. Therefore, we removed this statement totally.

3. *“Also, in the discussion, there is a statement: "This study yielded information on some of the first CM-specific transcriptomes, which will provide a valuable resource for researchers in the field." Again here, this point is not backed up by any data. Even though the data mentioned sequencing data were published previously elsewhere still the authors should provide at least some general results of single-cell sequencing to support their statements or rewrite the text accordingly to the content of this manuscript.” .”*

We agree with the reviewer's concern. Therefore, we removed this statement.

4. *"The authors compare three different aspect ratios AR1, AR7 and AR11, which all mimic diseased characteristics. What would be the best "healthy" control for any of the proposed shapes?"*

We refer the reviewer to the lines 76 to 84 of the introduction of the tracked version of the revised manuscript. Healthy CMs have been shown by several previous studies to have 5:1 to 7:1 AR. In DCM, the AR of CMs changes to 11:1, whereas in HCM, the AR alters to 1:1.

Regarding control cells – we refer the reviewer to our recent published study for more detailed discussion[1]. In that study, we used "*pre-patterned*" and "*unpatterned*" cells as controls of our approach[1]. Pre-patterned cells were lysed immediately after isolation, while the unpatterned cells were cultured cells that were allowed to take any shape and treated with the same maintenance media throughout the 72-h culturing period.

5. *"It was mentioned in the discussion that the sorting process takes 40 minutes. What are the chances that gene expression in individual cardiomyocytes will be affected by this procedure? There will be differences between a cell that was picked first with a cell that was picked last, regardless of the shape. Can authors comment on this?"*

We appreciate the reviewer's concern.

The 40-minutes sorting time starts with removing the media over the chip (line 354 of the tracked version of the revised manuscript) and continues with calibration of the coordinates, scanning of the whole chip, qualified-cell selection and TryplE treatment. The aforementioned steps that are equivalent for all cells last about 20 minutes. Therefore, the picked-time difference between first and last picked cells is roughly 20 minutes. Although, the 20 minutes time difference is more than timing of FACS sorting for sorting of cell suspension, it is not that long to change the gene expression profile and it is less than the 30 minutes timing, suggested by the Smart-Seq2 protocol[2].

Moreover, in order to remove the batch effect of time of picking, we recommend a recurring order of AR1, AR7 and AR11, while picking selected cells.

Minor Concerns:

1. *"It would be helpful to mention how many cardiomyocytes can be picked for sequencing purposes in one experiment (from how many P2 rats at the time) and how is batch to batch reproducibility."*

We agree that it is would be helpful to mention number of patterned neonatal rat CMs can be picked in each round for one chip. Therefore, we reflected this point in the revised manuscript on lines 394 to 396, as follows:
"*Finally, about 50 cells that is roughly one-third of the selected cells were successfully picked up from each chip."*

Regarding the batch effect:
Since on the one hand, it is possible to keep several chips exactly in the same condition, and on the other hand, and each round of sorting is dedicated to one chip, the batch effect between picked cells from different chips is highly unlikely, however, the authors haven't yet studied the chip to chip batch effect.

2. *"Shape-dependent and single-cell should be written with a dash."*

We thank the reviewer for this point and we fixed it in the revised manuscript.

References:

1 Haftbaradaran Esfahani, P. *et al.* Cell shape determines gene expression: cardiomyocyte morphotypic transcriptomes. *Basic Res Cardiol.* **115** (1), 7, (2019).

2 Picelli, S. *et al.* Full-length RNA-seq from single cells using Smart-seq2. *Nat Protoc.* **9** (1), 171-181, (2014).

Response to Reviewer #3:

Overall Comment:

"The manuscript presented by Payam Haftbaradaran Esfahani et al. established the protocol to collet primary CM at different shapes for scRNA seq, which was recently published on Basic Research in Cardiology. I have several concerns to the manuscript."

We thank the reviewer for her/his overall comments.

Major Concerns:

1. *"The reason why the cardiomyocytes shape changed in fibronectin-coated CYTOO chip should be specified."*

We appreciate the reviewer's point. Therefore, we clarified this point on lines 118 to 122 of the tracked version of the revised manuscript, as follows:
"The micropatterns were coated by fibronectin, surrounded by cytophobic surface. Therefore, CMs will attach, spread and capture the defined AR of its fibronectin micropattern by solely growing on the fibronectin substrate, while avoiding the cytophobic area."

2. *"The author chose neonatal rat cardiomyocyte as the model to study the shape effect in cardiomyopathies such as HCM and DCM. But overload caused cardiomyopathies mainly happen in adult and aged patients. Did the author try the adult cardiomyocytes?"*

We appreciate the reviewer's point and agree that cardiomyopathies happen in adult heart. However, as discussed on lines 389 and 390 of the discussion of the revised manuscript, it is exceptionally challenging to culture enough number of vital adult CMs for 72 hours in defined shapes. Moreover, as discussed on lines 144 to 146 of the introduction of the revised manuscript, the proposed approach was inspired by Kuo et al.[1], who used a similar approach and reported that they observed changes in physiological parameters due to changes in cell shape.

3. *"What is the size of the neonatal rat cardiomyocyte? How many cells could be plated in each well in the CYTOO chip?"*

Kuo et al.[1] found that the surface area of cultured neonatal rat CMs could reach to 2500 μm^2. The micropatterns used in this study had 2200 μm^2. However, this is the size of 72-hour cultured neonatal rat CM, not at the time of plating. The size of the just-plated neonatal rat CM is much less than 2200 μm^2.

Regarding the second part of the reviewer's question, we refer the reviewer to the line 122 of the introduction of the revised manuscript in which we discussed that "*the micropatterns are **not** in a well-shaped format. Instead, the fibronectin level is exactly at the same height of the surrounding cytophobic area*".

Regarding the number of cells could be plated on each micropattern (not well), we refer the reviewer to the lines 366 to 367 of the tracked version of the revised manuscript in which we discussed that "*the micropatterns were only selected if they contained a mononucleated single cell and only when the cell fully covered its fibronectin micropattern".*

4. *"For primary cells cultured in vitro, why does the author choose 72h, but not 24 or 48 hours? Does the changed transcription level come from both the shape and cell status? Did the author or others compare the gene expression level and the cell function in fresh cardiomyocyte and 72h cultured cardiomyocytes in such a system?"*

We appreciate the reviewer's concern. The proposed approach was inspired by Kuo et al.[1], who used a similar approach and reported that they observed changes in physiological parameters due to changes in cell shape in 72 hours. Moreover, the plated CMs need at least 48 hours to grow and completely capture the geometry of its micropattern substrate. Therefore, 72 hours seem logical to study the effect of cellular AR on gene expression.

In addition, the proposed method can be used to study the effect of different culturing time-course from 72 hours to one week, depending on the study cell type.

Regarding the last part of this reviewer's question, concerning the gene expression of freshly-isolated CMs, we refer the reviewer to our recent published study for more detailed discussion[2]. In that study, we used "pre-patterned" and "unpatterned" cells as controls of our approach[2]. Pre-patterned cells were lysed immediately after isolation, while the unpatterned cells were cultured cells that were allowed to take any shape and treated with the same maintenance media throughout the 72-h culturing period.

5. *"The introduction part is redundant. Please make it concise and clear."*

We completely agree with this reviewer's point and appreciate it. Therefore, we updated the introduction accordingly. In addition, some paragraphs reordered to create a concise flow of ideas.

Minor Concerns:

1. *"abbreviations in the introduction part should be specified."*

We thank the reviewer for this point. Some abbreviations are specified in the abstract that is why they are not specified again in the introduction. For example, AR, DCM and HCM are specified in the abstract.

References:

1 Kuo, P. L. *et al.* Myocyte shape regulates lateral registry of sarcomeres and contractility. *Am J Pathol.* **181** (6), 2030-2037, (2012).

2 Haftbaradaran Esfahani, P. *et al.* Cell shape determines gene expression: cardiomyocyte morphotypic transcriptomes. *Basic Res Cardiol.* **115** (1), 7, (2019).

Permission to re-use the figure

We re-used the "supplementatry figure 1" from our previous publication[1] to republish it as the figure 1 of our current manuscript to JoVE.

The link to the permission policy that allows to republish the figure:

https://link.springer.com/article/10.1007/s00395-019-0765-7#rightslink

a copy of the link is inserted here:

Rights and permissions

1 Haftbaradaran Esfahani, P. *et al.* Cell shape determines gene expression: cardiomyocyte morphotypic transcriptomes. *Basic Res Cardiol.* **115** (1), 7, (2019).